

CONF. 790133-7

LA-UR -79-76

**TITLE:** MATERIALS PROBLEMS WITH INERTIAL CONFINEMENT FUSION TARGETS

**AUTHOR(S):** Eugene H. Farnum  
R. Jay Fries  
James E. Barefield, II

**SUBMITTED TO:** First Topical Meeting on Fusion Reactor Materials  
Jan. 29-31, 1979  
Miami Beach, FL

NOTICE  
This report was prepared as part of the work under contract number W-7400-ENG-26 between the University of California and the United States Energy Research and Development Administration. The work was performed by the Los Alamos Scientific Laboratory, University of California, Los Alamos, New Mexico 87545.

By acceptance of this article for publication, the publisher recognizes the Government's (license) rights in any copyright and the Government and its authorized representatives have unrestricted right to reproduce in whole or in part said article under any copyright secured by the publisher.

The Los Alamos Scientific Laboratory requests that the publisher identify this article as work performed under the auspices of the USERDA.

  
**Los Alamos**  
**scientific laboratory**  
of the University of California  
LOS ALAMOS, NEW MEXICO 87545

An Affirmative Action/Equal Opportunity Employer

**MASTER**

## MATERIALS PROBLEMS WITH INERTIAL CONFINEMENT FUSION TARGETS\*

E. H. Farnum, R. J. Fries, J. Barefield II

University of California  
Los Alamos Scientific Laboratory  
Los Alamos, New Mexico 87545, USA

### INTRODUCTION

Inertial Confinement Fusion (ICF) reactors will irradiate pellets containing deuterium-tritium (DT) fuel to cause microexplosions at a rate of 1 to 20 Hz. While neither the driver nor the target design are presently specified, targets whose yields have been calculated to be adequate, are sufficiently similar in materials and configuration for many materials problems to become readily apparent. Because the plasma properties of target materials are most important during compression, target designs are optimized for these properties. However, this emphasis can create problems in target fabrication, for which, in contrast, the solid-state properties of materials are most important. For example, properties of interest in target design include average atomic number, highest and lowest atomic number, initial density, surface smoothness, and homogeneity, whereas the solid-state properties of interest are strength, hydrogen permeability and embrittlement, grain structure, exact chemical composition and stability, solubility, and melting point which strongly affect the fabrication techniques and the degree of difficulty in target preparation, as discussed below.

### TYPICAL LASER FUSION TARGET

The schematic shown in Fig. 1 is typical of high-yield targets designed at LASL for CO<sub>2</sub> laser drivers. In this target the DT fuel is frozen as a uniform layer onto the inside surface of the first, innermost, high-atomic-number (high-Z) shield shell which contains the fuel during hydrodynamic

---

\*Work supported by the U.S. Department of Energy.

compression. In the target shown this shell is made of tungsten or gold, 400  $\mu\text{m}$  in diameter with a 5- $\mu\text{m}$  thick wall. Current design for 20 TW laser irradiation specifies a solid DT layer thickness of up to 15  $\mu\text{m}$ , which requires a room-temperature gas pressure of 18.7 MPa inside the 400- $\mu\text{m}$ -diameter shell. Surface irregularities must be less than 10 nm both inside and outside and both diameter and wall thickness uniformity must be better than 1%. As a result of the surface-finish requirement, the shield shell cannot be filled with fuel gas through a permanently attached tube but must be filled by permeation at elevated temperature. Therefore, the first shell material must have the following properties: it must be applicable as a uniform, 5- $\mu\text{m}$ -thick coating onto microballoon mandrels with surface smoothness better than 10 nm (for present designs at 1- $\mu\text{m}$ -thick glass bubble liner for the metal shell is acceptable); it must be sufficiently permeable to hydrogen isotopes so that the shell can be filled by permeation in a reasonable time at temperatures that will not damage the coating; the material must be resistant to hydrogen attack so that neither strength nor surface smoothness are reduced by exposure at the temperature/pressure/time conditions of the fill; to hold 18.7 MPa of gas at room temperature, it must exhibit a tensile strength in excess of 374 MPa (55 000 psi); and it must have an atomic number equal to or greater than that of tungsten ( $Z = 74$ ).

The next outer layer in this target (Fig. 1) acts as a buffer or cushion between the two high-Z pusher shells to smooth hydrodynamic instabilities and to reduce shock-wave formation when the shells collide during the implosion. This cushion must be a low-density ( $\rho < 0.5 \text{ Mg/m}^3$ ), low-atomic-number (average  $Z < 4$ ), highly uniform (max size of irregularity,  $< 1 \mu\text{m}$ ) material. Either low-density small-cell plastic foam or gas is useful. However, plastic foam with a density of  $< 0.05 \text{ Mg/m}^3$  and a pore size of  $< 1 \mu\text{m}$  is very difficult

to fabricate<sup>1</sup>, and we are presently unable to produce such a foam in hemispherical shapes for the buffer. On the other hand, the only gas useful as a buffer at the cryogenic temperature (<20 K) necessary to create the solid DT fuel layer, is helium and even at this temperature, a pressure of  $\sim 0.2$  to  $0.5$  MPa (2 to 5 atm) is required to achieve a density of  $0.05 \text{ Mg/m}^3$ . In addition, supporting the inner pusher within this gas buffer without introducing defects  $>1 \text{ }\mu\text{m}$  in size is difficult while plastic foam provides easy support and centering.

Although surface-finish requirements for the outer pusher shell are less severe than for the high-Z shield, fabrication problems are more difficult because this shell probably will be made in hemispheres and assembled around the inner layers, and because a high-Z, low-density material is desired. High-Z metal is chosen as a radiation shield to prevent fuel preheat, and densities of  $1.3$  to  $3.0 \text{ Mg/m}^3$  are required to reduce the shell aspect ratio (diameter/wall thickness). Promising materials are metal-loaded plastics and metal foams. Inhomogeneities and surface defects of this shell must be less than  $1 \text{ }\mu\text{m}$  in diameter.

The absorber shell shown in Fig. 1 is presently unspecified. The material will be chosen to enhance laser light absorption, but dimensions and surface requirements await the results of future experiments. The presence of a vacuum annulus between absorber and outer pusher shell is also of unknown value but will be investigated in target optimization experiments. Because most materials problems are encountered in fabricating the high-shield of this target, we will discuss some of these problems in greater detail below.

#### MATERIALS PROBLEMS IN HIGH-Z PUSHER-SHELL FABRICATION

We have tried to fabricate targets which approach the size and strength limit required for the high-Z shield shell in Fig. 1. The shells used for our experiments were Solacels (Nickel-alloy microballoons  $1 \text{ mm}$  o.d. with  $1$  to  $2 \text{ }\mu\text{m}$  thick wall from Solar division of International Harvester Corp.),

with 25- to 50- $\mu\text{m}$ -thick coatings of gold or tungsten. We tried to fill these shells with 50  $\mu\text{g}$  of DT gas, which generates a room-temperature stress in a 25- $\mu\text{m}$ -thick wall of over 400 MPa (60 000 psi). Pure gold was applied to quality selected Solacels by electroplating from a sulfite electrolyte, and tungsten was applied by chemical vapor deposition of  $\text{WF}_6$  in hydrogen at 693 K in a fluid bed. The resulting shells were inspected by x-ray microradiography after coating to determine wall thickness and diameter and were studied for permeability by using 20 MPa (3 000 psi) of  $\text{D}_2$  gas at 923 K (650°C) for various lengths of time. Internal gas content was measured by crushing the microballoons in an evacuated, calibrated volume and measuring final pressure with a capacitance manometer. Gas composition was checked with a mass spectrometer connected to the calibrated volume through a leak valve. To measure bursting strength, we filled a batch of characterized microballoons to successively higher pressures and watched for explosion upon pressure release. The gas content of unexploded balloons was checked by statistical sampling using the destructive method described above. The electroplated gold coatings lost most of their strength and became porous when exposed to  $\text{D}_2$  gas at temperatures necessary for permeation fill<sup>2</sup>. To study the effect of hydrogen on gold coatings at permeation temperatures, several solacel substrates were coated with 25  $\mu\text{m}$  of CVD tungsten and then electroplated with 25  $\mu\text{m}$  of gold. These shells were then subjected to 20 MPa of  $\text{D}_2$  at 923 K for 5 days and were crushed to determine their gas content. A scanning-electron micrograph (SEM) of a typical fractured edge is shown in Fig. 2. The 2- $\mu\text{m}$ -thick Solacel is clearly visible as the innermost layer. Small blisters or bubbles appear to have caused separation between the solacel and the intermediate 25- $\mu\text{m}$ -thick tungsten layer. Metallographic sections and SEM micrographs taken before and after coating do not show any morphological changes in the tungsten layer. However, the outside layer, which originally consisted of 25  $\mu\text{m}$  of gold, had foamed to a

density about half of normal with pores as large as 10  $\mu\text{m}$ . This change was probably caused by decomposition of carbon and nitrogen compounds which were entrapped from the plating solution during the coating process.

Tungsten coatings maintained strengths in excess of 374 MPa (55 000 psi), but permeability decreased rapidly with increasing coating thickness. Figure 3 plots the measured fill rate at 923 K (650°C) for 25-, 31-, and 50- $\mu\text{m}$ -thick tungsten coating as well as the rate calculated from permeation data on wrought tungsten.<sup>3</sup> While the 25  $\mu\text{m}$  thick coatings show a higher permeation rate than wrought tungsten, the 50  $\mu\text{m}$  thick coatings are essentially impermeable and the 31  $\mu\text{m}$  thick coatings are nearly so. This is in sharp contrast to normal permeation behavior in which case the fill rate is inversely proportional to thickness. To investigate this effect we applied a 100  $\mu\text{m}$  thick CVD tungsten coating to a Solacel in two stages, crushed the microballoon and examined the fractured edge with an SEM. As shown in Fig. 4, the first  $\sim 20$   $\mu\text{m}$  consists of rather large (2  $\mu\text{m}$  diameter) columnar grains while the next  $\sim 40$   $\mu\text{m}$  has much smaller more randomly oriented grains. This behavior probably results from changing action in the fluid bed. Initially, the bed is rather light and colliding particles do not have enough mass to affect the grain growth. As the coating becomes thicker, however, the particle mass becomes large enough that interparticle collisions cause abrasion and generate nucleation sites thus reducing the grain size. Together with the permeation data, this suggests that the very fine grain CVD tungsten is nearly impermeable to hydrogen.

The desired fill was finally approached by diffusion-filling microballoons with 25- $\mu\text{m}$ -thick tungsten walls and subsequently overcoating the filled microballoons with electroplated gold. Because of temperature and pressure limitations in our tritium fill system we were only able to achieve a final DT gas content of 40  $\mu\text{g}$  in a 1.1-mm-i.d. target with 25- $\mu\text{m}$ -thick wall, which corresponds to a wall stress of 375 MPa. Furthermore, as shown in Fig. 2, we observed separation

between the Nickel alloy Solacel and the tungsten coating which was larger than the allowed 1- $\mu$ m inhomogeneity.

Therefore, even with CVD tungsten coatings several problems remain to be solved before high-Z pusher shells meet design specifications. Separation between the coating and the Solacel substrate must be eliminated. This will require either a careful analysis and elimination of the causes of bubbling and blistering or a change of substrates. Glass microballoon substrates are currently too small for the largest shells, but work to increase their size is in progress at several laboratories. We are also trying several techniques to form high-Z metal shells directly without a substrate. In addition, we are investigating other gold alloys and different plating techniques which may permit the use of gold-alloy coatings.

#### CONCLUSION

The selection and fabrication of materials for advanced laser fusion targets is a difficult task. It is complicated by the difference in physical properties that are important in design and in fabrication. We have seen that the hydrodynamic requirement for smooth surfaces dictates that the DT fuel be permeation-filled into the inner-shell materials, which must withstand exposure to high-temperature, high-pressure hydrogen without deterioration, and that the hydrogen permeability be in the correct range. In addition, we pointed out that the need to assemble complex targets after fuel fill requires that the inner shell withstand high internal pressure even though in the desired target configuration the fuel is frozen in place as a solid, cryogenic layer.

Gold and tungsten were investigated for use as inner, high-Z shells, and as yet unsolved problems were encountered with both materials. Pure electroplated gold lacks sufficient tensile strength to be useful by itself and in addition became porous foam when heated to 923 K in hydrogen. Tungsten, which can be deposited by chemi-

reduction of  $WF_6$ , does not show substantial morphological changes on exposure to hot hydrogen, but exhibits extremely low permeability to hydrogen in coatings thicker than 25  $\mu m$ . This low permeability limits the maximum achievable fuel content to an amount that can be contained by a shell with wall thickness  $\leq 25 \mu m$ .

Many other materials problems, to which we have alluded only briefly, are encountered in the fabrication of outer target layers. Although these problems are being attacked as vigorously as available staffing will permit within the inertial-confinement fusion program, a great deal of research and development must also be supported at independent laboratories before high-yield ICF targets can be fabricated.

We gratefully acknowledge the help of William McCreary and Sherman Armstrong in applying metal coatings and of Herman R. Maltrud in DT fill.



## REFERENCES

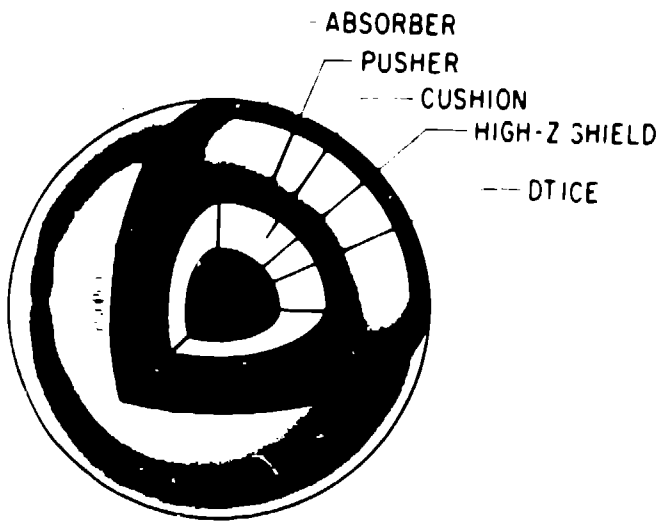
1. J. A. Rinde and R. R. Stone, "Preparation and Fabrication of Low Density Microcellular-Foam Laser Targets," Lawrence Livermore Laboratory report UCRL 51708 (Jan. 1975).
2. G. R. Gaskey and R. G. Derrick, *Scripta Met.* 10, 377 (1976).
3. W. G. Perkins, *J. Vac. Sci. Technol.* 10, 543 (1973).

Fig. 1. Cutaway drawing of a typical high gain laser fusion target.

Fig. 2. Scanning-electron micrograph of a fractured surface of a 2- $\mu\text{m}$ -thick Solacel coated with 25  $\mu\text{m}$  of CVD tungsten plus 25  $\mu\text{m}$  of electroplated gold and heated to 923 K in 20 MPa of  $\text{D}_2$  for 5 days. 500X

Fig. 3. Fill rate data for CVD tungsten shells at various coating thicknesses. filled by permeation with  $\text{D}_2$  gas at 923 K, 20 MPa. Data points indicate measured rates, lines without points are rates calculated using the permeability of wrought tungsten.

Fig. 4. Scanning-electron micrograph of the fractured surface of a 100  $\mu\text{m}$  thick CVD tungsten coating on a Solacel. Only the inner  $\sim 60 \mu\text{m}$  is shown.



OVERALL DIAMETER  $\approx 2$  mm

Fig 1



Fig 3

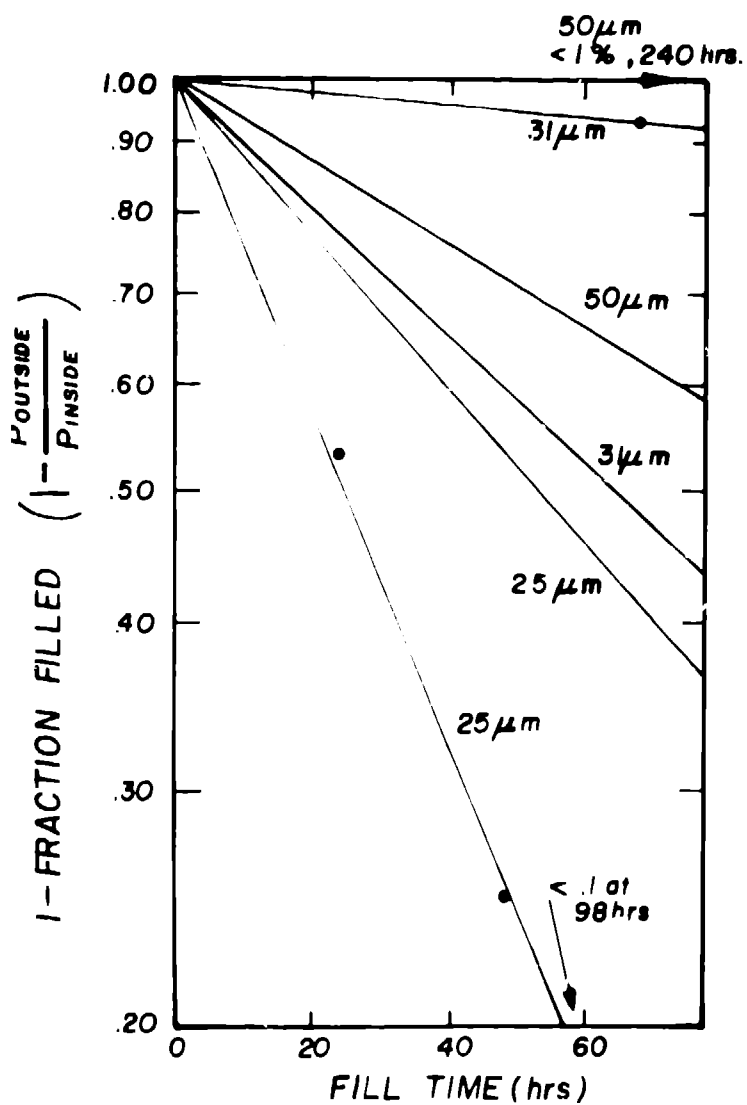


Fig 2



Fig 4